Rapid thermal equilibration of differentially heated protein and water in bovine corneal stroma

George Alexander Marcus[*]
Department of Physics and Astronomy, 1 College Circle, SUNY Geneseo, Geneseo, New York 14425, USA

H. Alan Schwettman[†]
Department of Physics, 382 Via Puebla Mall, Stanford University, Stanford, California 94305-4060, USA

(Received 18 July 2011; revised manuscript received 9 August 2011; published 13 October 2011)

We measure and simulate the thermal response of bovine corneal stroma to a picosecond IR heating pulse. A thermal diffusion model is developed for this tissue based on the spatial distribution and properties of protein and water constituents in the stroma. In this idealized model, differentially heated protein and water constituents thermally equilibrate with a thermalization time of 515 ps. Using transient absorption spectroscopy for picosecond protein thermometry, a significantly faster thermalization time of 165 ps is measured. The implications of this faster than expected thermalization for the energy-partition model of short-pulse mid-IR tissue ablation are discussed.

DOI: 10.1103/PhysRevE.84.041913 PACS number(s): 87.50.W−, 44.05.+e

I. INTRODUCTION

The study of laser-tissue interaction is important in the development of biomedical applications of laser technology. Laser ablation as a precision cutting tool is one such application. Key metrics that determine the practical viability of laser ablation are the precision of the cuts and the type and extent of collateral damage beyond the cutting zone. A detailed understanding of the mechanisms of laser-tissue interaction and the tissue ablation process is critical for improving laser ablation techniques [1].

In a standard model for laser ablation of tissue, material removal is driven by explosive vaporization of the water. When the water in the tissue reaches the superheating limit, water vapor bubbles grow, straining the tissue structural proteins until they mechanically fail and release the accumulated stress energy. Mid-infrared laser pulses for ablation in the thermal confinement time regime can selectively deliver energy to strong vibrational modes with short penetration depths in the tissue constituents leading to a combination of excellent cutting precision and ablation efficiency. Edwards *et al*. reported that despite comparable penetration depths, ablation pulses tuned to the amide I and II bands (1660–1550 cm^{-1}) in protein resulted in enhanced ablation efficiency and reduced collateral damage relative to pulses tuned to the strong water stretch band at 3300 cm^{-1} [2]. Later studies have examined tissue ablation using IR lasers [3–7] and the efficacy of different IR laser sources for ablation [8–10]. The difference in ablation efficiency measured by Edwards cannot be explained by applying the standard ablation model to the average tissue properties.

Hutson *et al*. proposed an "energy-partition" model, which takes into account the different optical, thermal, and mechanical properties of the protein and aqueous constituents of tissue [11]. They suggest that differential heating of these constituents accounts for the wavelength dependence of the ablation efficiency. In their model, the differences in the penetration depth, density, heat capacity, and thermal conductivity of the tissue's protein relative to its water transiently yield different average temperatures for the spatially separated constituents of this highly structured tissue. The large thermal mass of the tissue water suggests that under thermal confinement conditions, the average protein temperature can be substantially higher than the average temperature until the protein and water thermally equilibrate. Assuming that protein denaturation is an Arrhenius type process [12], the elevated protein temperature may result in the denaturation of a fraction of the structural protein. When explosive vaporization occurs, brittle denatured protein fractures more easily than normal protein, releasing less strain energy and causing reduced collateral damage.

If this model is correct, an optimal ablation pulse would maximize the denaturation fraction of the structural proteins while still causing explosive vaporization of water to drive the material removal process. In the mid-IR, where both protein and water have strong absorptions, an ideal wavelength for an ablation pulse would satisfy two conditions: (1) a large ratio of protein absorption to water absorption so that the differential heating will lead to significant protein denaturation, and (2) a sufficiently large total absorption to drive explosive vaporization. The optimal length for the ablation pulse will depend on the time scale for thermal equilibration between the protein and water components of the tissue. If the pulse is too short, there will be insufficient time to accumulate significant thermal damage. If the pulse is too long, thermalization between the protein and water will increase the average water temperature. The effect of the elevated average protein temperature would be counteracted by the fact that the water would reach the superheating limit more rapidly, allowing less time for the accumulation of thermal damage to the protein.

II. MODEL OF THERMAL DIFFUSION IN BOVINE STROMA

We use bovine corneal stroma to examine thermalization of differentially heated tissue components because it is well

[*]marcus@geneseo.edu
[†]has@stanford.edu

 ©2011 American Physical Society

characterized and has a highly ordered structure. A thermal model of the tissue was developed to predict the rate of thermalization between its protein and water constituents.

A. Structure of corneal stroma

The stroma, one of five layers of the cornea, constitutes the bulk of corneal tissue. At physiological hydration, bovine stroma is 76% water, 23% protein, and 1% lipids by mass. The majority of the protein mass (75%) is in the form of collagen [13], most of which exists as ordered collagen fibrils made primarily of type I collagen with a small quantity of type V collagen. Type I collagen is composed of three 3_{10}-helical polypeptide chains that are themselves arranged in a triple helix, forming a coiled-coil structure that results in a rod-shaped molecule 1.5 nm in diameter and 300 nm long [14]. The collagen molecular structure is stabilized via internal-hydrogen bonding as well as water-bridged bonding between adjacent chains. Individual collagen molecules aggregate both laterally and longitudinally into intermediate microfibril structures, typically 4 nm in diameter with molecules spaced 1.8 nm apart [15]. The microfibrils aggregate into larger fibril bundles driven by crosslinks between the nonhelical terminal regions of adjacent collagen molecules. The hierarchy of collagen structure is displayed in Fig. 1.

In bovine stroma, x-ray diffraction measurements [16,17] show that uniform fibrils, 38.2 ± 2 nm [18] in diameter, pack in a hexagonal pattern with a center-to-center fibril spacing of 62.5 ± 4.9 nm. The extrafibrillar matrix consists primarily of water. The hexagonally packed fibrils are aligned in 1–2-μm-thick layers called lamellae with adjacent lamellae oriented with nearly orthogonal fibril axes. Though the stroma is not crystalline, it does exhibit short-range order, which is critical to maintaining the transparency to visible light that is an integral part of stromal function.

Water exists in three forms in fibrillar tissue. Structural water is found in the collagen in stoichiometric quantities and plays a fundamental role in the collagen helical stability. Bound water fills the gaps between molecules in the microfibrils and between the microfibrils in the fibrils. Though these "bound" waters are not directly bound to any particular molecular hydrogen-bonding site, they do not display the same properties as free water. Finally, free water, which constitutes 75% of the water in stromal tissue, is located between fibrils [19].

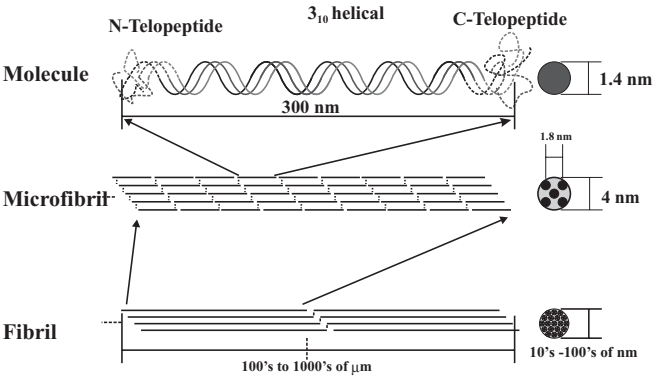

FIG. 1. Hierarchy of collagen organization from molecule to fibril.

B. Thermal diffusion model in stroma

To determine the time scale for thermal equilibration between the protein and water constituents of corneal stroma, we must solve the thermal diffusion problem in a model of corneal stroma in which the spatially separated protein and water constituents have been differentially heated. Such a model simulates an experiment in which a short mid-IR heating (or ablation) pulse delivers a thermal impulse to the tissue. The stromal structure is idealized as a periodic hexagonal lattice with collagen fibrils on the lattice points and water in the extrafibrillar spaces. A simplifying assumption is that the fibrils are composed purely of collagen, ignoring the presence of structural and bound water. This simplified model is reducible to two dimensions because the nanometer-scale spacing between and transverse dimensions of the fibrils is much smaller than the typical fibril length of 500 μm [20]. The characteristic length scale of the fibrils is also smaller than the sample thickness and optical penetration depth, both of which are on the scale of a few microns. This means that thermal energy diffuses along the long fibril axis slowly relative to the transverse thermal diffusion and thus variation along the longitudinal axis can be ignored.

A schematic of the geometry used for the model is shown to scale in Fig. 2 with dark gray circles representing the collagen fibrils and light gray shading showing the extrafibrillar region filled with water. The sixfold symmetry of the system means that there is no heat flow across the boundaries of the triangle ABC indicated in the figure. The full temperature distribution is found by calculating thermal diffusion in the triangular region while treating the triangle's edges ABC as insulating boundaries.

The temperature distribution is found using finite-element methods in the triangular region to solve Fourier's equation,

$$\rho C_p \frac{\partial T}{\partial t} = k\nabla^2 T + Q, \tag{1}$$

in which ρ is the density, C_p is the heat capacity at constant pressure, T is the temperature, k is the thermal conductivity, and Q is the heat source term that represents the pump laser pulse.

Because the heat source in the model is a thermal impulse, Q is represented by a δ function at time $t = 0$ scaled to the pump pulse energy. The problem then reduces to a

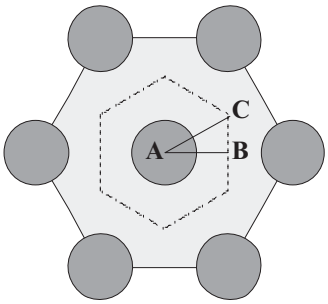

FIG. 2. Geometry of the idealized model of corneal stroma used for the finite-element model of thermal diffusion. The dotted hexagon is the unit cell of the hexagonal lattice. The triangle ABC is the smallest bound region that contains all of the information needed to reconstruct the full spatial distribution of temperatures.

TABLE I. Mechanical and thermal parameters of stromal constituents.

Parameter	Water	Collagen
ρ (kg/m^3)	1000	1540
C_p [J/(kg K)]	4184	1560
k [W/(m K)]	0.602	see text

homogeneous problem with two different materials at different initial temperatures in contact with each other. The thermal contact resistance at the interface between the collagen and water is assumed to be zero. This assumption yields a lower limit for the thermalization time. Since thermal diffusion depends linearly on the temperature difference between the collagen and water regions, the initial temperature difference between the constituents can be arbitrarily scaled without loss of generality. Finally, although Fourier's equation implicitly assumes an infinite velocity for thermal wave propagation, Hutson *et al.* [11] showed that properly accounting for a finite propagation velocity is only important for the initial few picoseconds of dynamics. This time scale is much smaller than the transverse thermal diffusion time scale and is not relevant for this study.

The results of the model depend heavily on the heat capacity, density, and thermal conductivity of the stromal constituents. With the exception of the thermal conductivity of collagen, these parameters can be found in the literature and are shown in Table I.

Determining the thermal conductivity of a protein like collagen is challenging. Though there is no consensus value in the literature for the thermal conductivity of pure collagen, there is a range of values for tissues that are composed primarily of collagen. Once the thermal conductivity of the heterogeneous tissue is measured, taking into account assumptions about the contact resistance, an approximate value for k of the protein can be extracted using the assumption [21] that each tissue constituent contributes to the total thermal conductivity proportional to its mass fraction in the tissue. This assumption yields the result that the thermal conductivity for collagen that is likely to be between 0.195 W/(m K) [22] and 0.400 W/(m K) [23]. In the model, a value of 0.300 W/(m K) is used and the influence of this parameter on the thermalization time is determined.

C. Results of the model

The temporal and spatial progression of the thermalization process is visualized in Fig. 3 by plotting the temperature along the fiducial symmetry line AB indicated in Fig. 2. It should be noted that this is a radial slice of a nearly cylindrically symmetric system so the scaling of volume with distance from the origin (at A) is lost.

From the time-dependent, two-dimensional distribution of temperatures over the unit cell of the tissue system, we can find the average temperature of the protein and of the water in the tissue. The thermalization time is determined by fitting the time-dependent average temperatures to a biexponential decay,

$$T(t) = A_{\text{slow}} e^{-t/\tau_{\text{slow}}} + A_{\text{fast}} e^{-t/\tau_{\text{fast}}} + A_{\text{eq}}, \qquad (2)$$

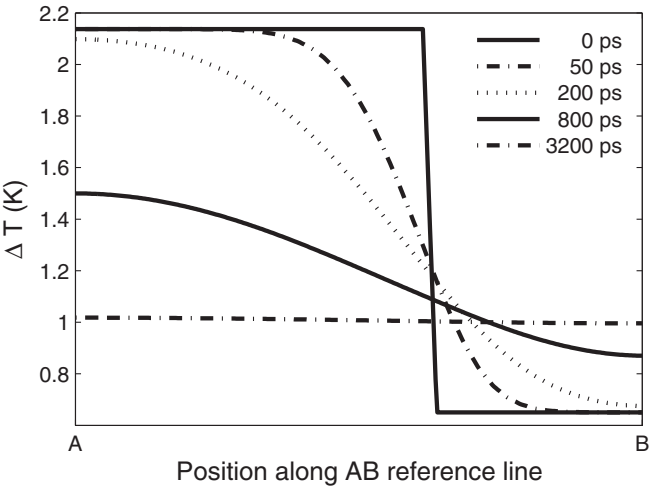

FIG. 3. The temperature along the line AB at various delay times after the initial excitation assuming $k_{\text{fibril}} = 0.300$ W/(m K). The position of the interface between the collagen fibril and H_2O extrafibrillar matrix is apparent in the initial $t = 0$ temperature profile.

with fast and slow decay components. It should be noted that this model is used purely for simplicity as there is no physical mechanism directly indicating a biexponential system. The difference between a single and biexponential model is discussed further below. A calculated thermalization curve for the average temperature of the collagen and water following a thermal impulse is shown in Fig. 4 along with a fitted decay. The best fit parameters are shown in Table II.

The relative amplitudes of the slow and fast decay components indicate that the amplitude of the slow component dominates the temperature curve. A model with a single exponential decay was also examined and though the fit was less satisfactory, the decay time closely paralleled the slow decay time. Therefore we assume that the slow decay time

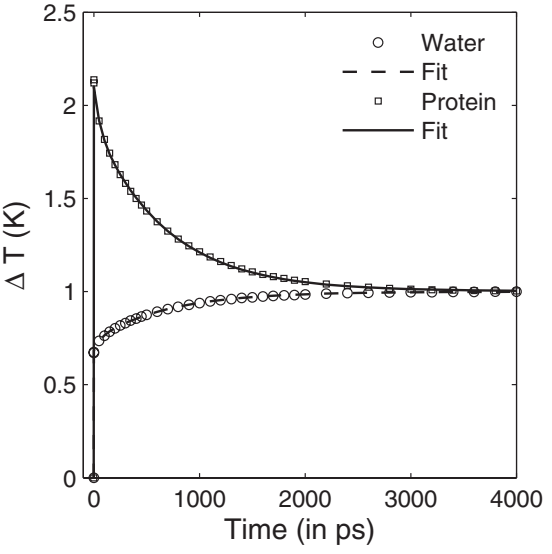

FIG. 4. Modeled temporal evolution of the average fibril and water temperatures calculated for $k_{\text{fibril}} = 0.300 \frac{\text{W}}{\text{mK}}$. The points represent the simulated thermalization data and the lines are the biexponential fits to the simulated data.

TABLE II. Fit parameters for the data in Fig. 4.

Parameter	Fibril	Water
A_{slow} (K)	3.23 ± 0.01	-0.394 ± 0.014
τ_{slow} (ps)	516 ± 3	516 ± 3 ps
A_{fast} (K)	0.71 ± 0.01	-0.087 ± 0.002
τ_{fast} (ps)	42 ± 2	42 ± 2 ps
A_{eq} (K)	2.6 ± 0.001	2.6 ± 0.001

corresponds to the thermalization time that is measured experimentally. Although there are physical processes occurring on shorter time scales (like molecular vibrations and structural changes) the focus of this study is the redistribution of heat energy, which is best characterized by the long time scale. The thermalization time extracted from the model is strongly dependent on the thermal conductivity of the collagen that is a model input. Given the uncertainty in this quantity, the influence of this parameter on the thermalization time was calculated and is displayed in Fig. 5.

III. MEASURING THE THERMALIZATION OF DIFFERENTIALLY HEATED STROMAL CONSTITUENTS

Physiologically hydrated samples of corneal stroma are created from cryosectioned stroma by rehydrating them with pure water and placing them in a closed chamber maintained at 100% relative humidity at room temperature. The samples are allowed to soak in the humidity chamber until IR transmission measurements show that the IR water-to-protein absorption ratio had reached the physiological level, at which time the sample cells are permanently sealed. The stroma samples were mounted in a sample cell which maintained a constant temperature and relative humidity, ensuring uniform sample hydration during the course of the experiment [24].

To measure thermalization between hexagonally packed collagen fibrils and free water in corneal stroma, we use a two-color, mid-IR pump mid-IR probe spectroscopy technique. The pump pulse provides a thermal impulse, differentially heating the collagen and water based on their relative absorption. The probe pulse monitors infrared absorbance changes in order to measure temperature changes. This thermometry technique, described in detail elsewhere [24], uses rapid thermal shifts of IR absorption lines as a secondary thermometer. The thermal line shift equilibrates in a few picoseconds allowing temperature measurements on time scales longer than this. Absorption in the water association band, from 1900 to 2500 cm^{-1}, varies linearly with temperature due to changes in hydrogen bonding. As there are no protein absorption lines in this wavelength region, this is an excellent spectral window for measuring the average temperature of free water in the tissue. To monitor the average temperature of the protein constituent, we measure changes in absorption in the vicinity of 1590 cm^{-1}, in between the amide I and II bands. Because the protein absorption changes linearly with temperature in the small perturbation limit, transient absorption changes directly represent transient temperature changes. In this wavelength window, the absorption due to the water bend mode is nearly independent of temperature changes.

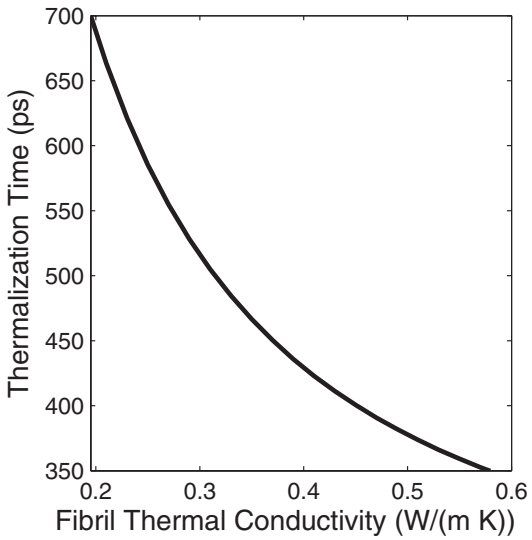

FIG. 5. The decay of the average fibril temperature is modeled for different values of fibril thermal conductivity.

The initial temperature jump and the equilibrium temperature induced in the constituents by the heating pulse are calculated using the optical and thermodynamic properties of the protein and water. These calculated temperature jumps, combined with the temperature dependence of the absorption coefficient measured by Fourier transform infrared (FTIR) spectroscopy, yields the expected initial and equilibrium transient absorption values. The measured optical absorption transients are fitted to the biexponential model with a term for the initial rapid transient jump attributable to the heating pulse and a subsequent slow relaxation, attributed to the thermalization of the tissue constituents. The amplitudes of the initial response, A_{init} is equivalent to the sum of the fast and slow responses, $A_{fast} + A_{slow}$, in the model. The equilibrium response A_{eq} along with the time scale for the equilibration between the temperatures of the protein and water constituents of the tissue, τ_{eq}, are extracted from the data. As indicated in the examination of the model, the slow decay time dominates the equilibration.

A 1-ps-long heating pulse is delivered at 1681 cm^{-1} in the amide I absorption band. This excitation wavelength provides a good match between the optical penetration depth of 6.9 μm and the sample thickness of 6.4 μm. At this wavelength, energy is deposited into both the H_2O bend mode and the protein amide I mode. Given the laser parameters, an initial jump in the protein temperature of $\sim$6.7 °C above baseline is expected. Once the differentially heated protein and water thermalize, an equilibrium tissue temperature of $\sim$2.6 °C above baseline is expected.

Although a probe pulse at the water isobestic point reveals the temperature changes solely in the protein, the expected difference in the initial and equilibrium protein temperatures is comparable to the sensitivity of the experiment, preventing an accurate measurement of time scale for the thermal equilibration between the protein and the water. However, measurements indicate that the initial and equilibrated protein temperature changes agree with the expected values. A larger protein response and an improved signal-to-noise ratio is

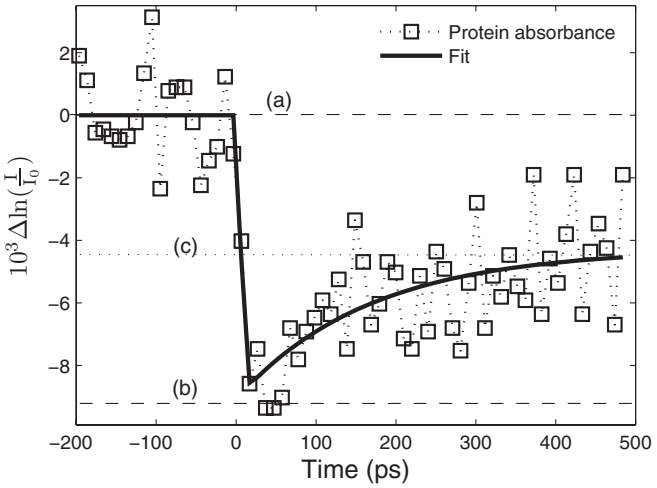

FIG. 6. Thermalization of stromal protein measured at 1570 cm^{-1} on the blue side of the amide II absorption in collagen following heating pulse at 1680 cm^{-1} in amide I. The horizontal lines represent the change in protein absorbance (a) preceding the arrival of the heating pulse, (b) immediately after the thermal impulse, and (c) after the temperature of the protein and water in the tissue have equilibrated.

observed by probing at 1570 cm^{-1} [24] where changes in the protein absorbance are significantly larger. However, at this wavelength some of the transient absorption response is due to temperature dependent changes in water absorption. The water adds a detectable offset to the amplitude of the absorption response, but has no effect on the time scale for thermalization as conservation of energy requires that the thermalization time must be identical for the water and protein equilibrating with each other. The equilibration of the protein absorbance (and temperature) is clearly visible in the transient absorption response in Fig. 6. The parameters of the measured protein thermalization, compared to predictions, are presented in Table III. The initial and equilibrium absorption changes are in excellent agreement with the predicted values. However, thermalization occurs on a time scale which is significantly faster than the thermalization time predicted by either the heat-diffusion model presented in this paper or the layer model suggested by Hutson *et al.* [11]. This is an issue that is examined in the results section.

The complementary measurement of the transient response of water in the tissue is made at a probe wavelength of 2150 cm^{-1}. The transient absorption scan appears in Fig. 7(a) with the thermalization parameters shown in Table IV. Once again, the amplitudes of the initial and equilibrium responses agree with the predictions. Although the initial response is larger than predicted and the equilibrium response is smaller

TABLE III. Protein thermalization parameters extracted from data in Fig. 6 compared to predictions.

	Measured	Predicted
A_{init}	$-8.9\ (+1.3/-2.6)\times10^{-3}$	-7.2×10^{-3}
A_{eq}	$(-4.6\pm1.8)\times10^{-3}$	-4.9×10^{-3}
τ_{eq}	165 (+150/−80) ps	516 ± 3 ps

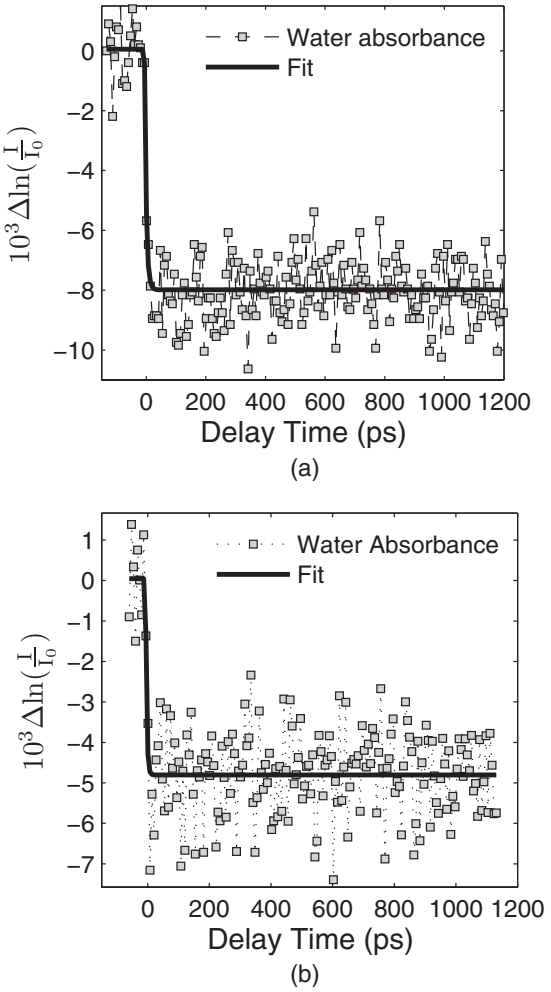

FIG. 7. Thermalization of stromal water measured at 2150 cm^{-1} following heating pulse (a) at 1680 cm^{-1} in amide I band or (b) at 1550 cm^{-1} in amide II band.

than predicted, these deviations are within the measurement uncertainty, making it difficult to draw further conclusions. Given the small difference between the initial and equilibrium values, it is not possible to measure the thermalization time scale.

Repeating the experiment with the heating pulse tuned to the amide II mode at 1550 cm^{-1} results in a smaller total absorption change than with amide I pumping, due to a smaller absorption coefficient in the stroma at this pump

TABLE IV. Water thermalization parameters extracted from data in Fig. 7 compared to predictions.

	Measured	Predicted
	Pumping amide I band	
A_{init}	$(-8.7\pm1.35)\times10^{-3}$	-7.4×10^{-3}
A_{eq}	$(-8.0\pm1.3)\times10^{-3}$	-7.9×10^{-3}
	Pumping amide II band	
A_{init}	$(-4.8\pm1.3)\times10^{-3}$	-2.7×10^{-3}
A_{eq}	$(-4.8\pm1.3)\times10^{-3}$	-5.3×10^{-3}

wavelength. However, since a larger fraction of the energy is deposited in the protein, the differential heating should be more pronounced. The measured transient absorption is displayed in Fig. 7(b) with the thermalization parameters also appearing in Table IV. There is a discrepancy between the measured and predicted amplitude of the initial absorption response. However, the amplitude of the measured change in absorbance is in agreement with the expected water response *after* thermalization and there is no indication of thermalization occurring on a time scale comparable to what was observed in the protein. The absence of a measurable thermalization signal in the water is discussed in the results.

IV. DISCUSSION OF RESULTS

There are two major discrepancies between the thermalization measurements and the heat diffusion model. The 516-ps thermalization time predicted by the model is much slower than thermalization time of 165 (+150/−80) ps measured in the stromal tissue. Additionally, the thermalization amplitude of the water response was too small to be measured, which is also inconsistent with the model.

The model has two primary sources of error: errors in the parameters used in the model and problems arising from the simplifications used in developing the model. Most of the input parameters for the model are well established in the literature. The uncertainty in the fibril diameter and spacing is small and has little influence on the calculated thermalization time. However, the thermalization time is very sensitive to the thermal conductivity of the protein, which is the only input parameter poorly characterized in the literature. Heterogeneous tissue must have a lower thermal conductivity than pure water, meaning that the thermal conductivity of protein has an upper bound of 0.600 W/(m K). As demonstrated in Fig. 5, at this extreme limit the thermalization time from the model is 345 ps, which is still slower than measured thermalization time. This suggests that, although the uncertainty in the value of the protein thermal conductivity may contribute to the discrepancy between the measured and modeled thermalization time, it is insufficient to fully reconcile the two.

There are two major idealizations in the model that are relevant to this issue. In the model, it is assumed that the collagen fibrils are composed purely of collagen and contain no structural or bound water. However, some studies suggest that as much as 63% of the volume of the hydrated fibril is actually composed of water [25]. The presence of water in the fibrils increases the thermal mass of the fibril volume, reducing the thermal mass ratio between the fibrillar and the extrafibrillar volumes. A hydrated fibril has a larger effective thermal conductivity. Finally, the close proximity of the water and collagen in the fibril shrinks the characteristic dimension for thermalization within the fibril to the 1–2-nm size scale of collagen molecules instead of the 40-nm scale of collagen fibrils. The average hydrated fibril temperature (which now includes water and protein) rapidly thermalizes to a lower temperature than the idealized protein fibril. The hydrated fibril then equilibrates with the extrafibrillar matrix on a slow time scale determined by the fibril diameter. This new model would be equivalent to the idealized model, with the protein parameters used for the fibril replaced by "effective" fibril parameters that combine the properties of the collagen and the bound water. However, the water's impact on the fibril's effective thermal conductivity counteracts the impact on the effective thermal mass, leaving the thermal diffusivity of the hydrated fibril largely unchanged. In summary, including water in the fibril generates a very fast component to the thermal response (on the time scale of a few picoseconds) and reduces the amplitude of the thermalization response in the fibril, but it fails to bring the thermalization *time* into agreement with the experimental results.

A second idealization in the model assumes that all of the protein in the stroma is located in the collagen fibrils. However, studies [25] suggest as much as 45% of stromal protein is found in the extrafibrillar matrix in the form of proteoglycans and nonfibrillar collagens. As with the composite fibril, the presence of extrafibrillar protein in the matrix leads to an "effective" extrafibrillar matrix that has properties in between those of the water and the protein, resulting in a reduced amplitude in the thermalization signal measured in the water. This reduced amplitude, in conjunction with the detection limitations of the experimental apparatus, can explain why no thermalization signal was detected in the transient absorption response of the water. The complementary reduction in the amplitude of the protein response could still be consistent with the measurement due to the sizable error bars on the measured amplitude.

The exact impact of extrafibrillar protein on the thermalization time is difficult to quantify as it strongly depends on the spatial distribution of the protein in the extrafibrillar space. In general, extrafibrillar protein reduces the average distance between the "hot" proteins and the "cool" water. It is likely that a thermal diffusion model of corneal stroma that more realistically accounts for the true spatial distribution of protein and water in the tissue will be in better agreement with the measurements, both with respect to the predicted thermalization time and the amplitude of the water thermalization response. Although corneal tissue is highly structured, it does not behave in a way that is consistent with an overly simplified physical model. Predictions based on an idealized structure must be treated with caution.

V. CONCLUSIONS

Our measurements indicate that thermalization of the constituents of stromal tissue occurs on a time scale that is substantially faster than predicted either by our idealized model or the one put forth by Hutson *et al*. [11]. Although our results support the idea that mid-IR heating pulses can generate a temperature difference between the tissue constituents, the measured thermalization between the tissue constituents is much faster than predicted. This suggests that differential-heating models of stroma must be revised to reduce the level of idealization in the model of tissue structure. In Arrhenius rate calculations of thermal damage to corneal protein, rapid thermal equilibration between the protein and water dramatically reduces the protein damage accumulated prior to the onset of ablation. This shrinks the potential operational parameter space for a mid-IR ablation mechanism,

which relies upon protein structural weakening to reduce collateral damage.

It must be noted that these thermal equilibration measurements were made in the limit of "small" temperature changes. It is possible that the thermalization behavior changes when the heating pulse is strong enough to cause explosive vaporization in the thermal confinement limit. For example, a strong heating pulse might vaporize the surface layer of water surrounding a "hot" fibril [26]. Since the thermal conductivity of water's vapor phase is an order of magnitude less than that of its liquid phase [27], this would thermally disconnect the fibril from the water. Such a thermal disconnect increases the thermalization time, allowing the protein to accumulate more thermal damage. Incorporating a vapor layer surrounding the collagen into our heat diffusion model, we find that the predicted thermalization time only increases by 30%, indicating that the effect is not dramatic. Nonetheless, the necessary presence of a vapor bubble during tissue ablation suggests the need to include the effects of vapor formation in the thermal diffusion models in tissue as small changes in the temperature as a function of time result in dramatic changes in the expected accumulation of damage calculated from the Arrhenius rate equation.

ACKNOWLEDGMENTS

This work was supported by the Air Force Office of Scientific Research, Grant No. FA 9550-04-1-00-75. We also acknowledge the support of the staff of the Stanford FEL center.

[1] A. Vogel and V. Venugopalan, Chem. Rev. **103**, 577 (2003).
[2] G. Edwards *et al*., Nature (London) **371**, 416 (1994).
[3] J. I. Youn, P. Sweet, G. M. Peavy, and V. Venugopalan, Laser. Surg. Med. **38**, 218 (2006).
[4] Y. Xiao, M. Guo, K. Parker, and M. S. Hutson, Biophys. J. **91**, 1424 (2006).
[5] M. S. Hutson, B. Ivanov, A. Jayasinghe, G. Adunas, Y. Xiao, M. Guo, and J. Kozub, Opt. Express **17**, 9840 (2009).
[6] K. Franjic, M. L. Cowan, D. Kraemer, and R. J. D. Miller, Opt. Express **17**, 22937 (2009).
[7] V. A. Serebryakov, E. V. Boiko, N. N. Petrishchev, and A. V. Yan, J. Opt. Technol. **77**, 6 (2010).
[8] M. A. Mackanos, D. Simanovskii, K. M. Joos, H. A. Schwettman, and E. D. Jansen, Laser Surg. Med. **39**, 230 (2007).
[9] G. S. Edwards, R. D. Pearlstein, M. L. Copeland, M. S. Hutson, K. Latone, A. Spiro, and G. Pasmanik, Opt. Lett. **32**, 1426 (2007).
[10] J. Kozub *et al*., Biomed. Opt. Express **2**, 1275 (2011).
[11] M. S. Hutson, S. A. Hauger, and G. Edwards, Phys. Rev. E **65**, 061906 (2002).
[12] R. Brinkmann, J. Kampmeier, U. Grotehusmann, A. Vogel, N. Koop, M. Asiyo-Vogel, and R. Birngruber, Proc. SPIE **2681**, 56 (1996).
[13] I. Fatt and B. A. Weissman, *Physiology of the Eye: An Introduction to the Vegetative Functions* (Butterworh-Heinemann, Boston, 1992).
[14] G. N. Ramachandran and A. Reddi, *Biochemistry of Collagen* (Plenum, New York and London, 1976).
[15] K. M. Meek and C. Boote, Exp. Eye Res. **78**, 503 (2004).
[16] D. W. Leonard and K. M. Meek, Biophys. J. **72**, 1382 (1997).
[17] K. M. Meek and N. J. Fullwood, Micron **32**, 261 (2000).
[18] K. M. Meek and A. J. Quantock, Prog. Retin. Eye Res. **20**, 95 (2001).
[19] A. Traore, L. Foucat, and J. Renou, Biopolymers **53**, 476 (2000).
[20] D. F. Holmes and K. E. Kadler, J. Mol. Biol. **345**, 773 (2005).
[21] H. Poppendiak, R. Randall, J. Breeden, J. Chambers, and J. Murphy, Cryobiology **3**, 318 (1966).
[22] J. Kampmeier, B. Radt, R. Birngruber, and R. Brinkmann, Cornea **19**, 355 (2000).
[23] A. Bhattacharya and R. Mahajan, Physiol. Meas. **24**, 769 (2003).
[24] G. A. Marcus and H. A. Schwettman, J. Phys. Chem. B **111**, 3048 (2007).
[25] D. W. Leonard and K. M. Meek, Biophys. J. **72**, 1382 (1997).
[26] C. P. LIn and M. W. Kelly, Appl. Phys. Lett. **72**, 2800 (1998).
[27] W. E. A. Wagner, J. Eng. Gas Turb. Power **22**, 150 (2000).